JOURNAL OF GEOPHYSICAL RESEARCH, VOL. 92, NO. C2, PAGES 1637–1654, FEBRUARY 15, 1987

Structure of the Coastal Current Field off Northern California During the Coastal Ocean Dynamics Experiment

P. MICHAEL KOSRO

College of Oceanography, Oregon State University, Corvallis

For 74 days during the spring and summer upwelling seasons of 1981 and 1982, in conjunction with the Coastal Ocean Dynamics Experiment, profiles of upper ocean currents were collected in the waters over the shelf and slope off northern California using a shipboard Doppler acoustic log. These measurements provide detailed information on the spatial structure of the current field. Synoptic maps of near-surface currents often deviate substantially from classical two-dimensional wind-driven upwelling and indicate a close association between the complex temperature structures observed in satellite imagery and the presence of vigorous current structures including squirts (regions of intense seaward flow), eddies, and countercurrents. Well-defined examples of a squirt and of a countercurrent during a cessation of wind forcing (wind relaxation event) are examined in detail. Despite this complexity, the nearshore synoptic current field was found to be anisotropic, varying more rapidly cross shore than alongshore. The structure of the current averages and simple fluctuation statistics were largely as deduced in other upwelling areas from moored measurements. A surface-intensified equatorward jet was found in the average alongshore currents, with vertical shear exceeding -2×10^{-3} s^{-1} over much of the shelf. The core of the jet moved offshore south of Point Arena and was better resolved in along-isobath averages. At depths below 80 m the average alongshore flow reversed, giving way to a poleward undercurrent, strongest near the shelf break. The detailed structure of the inferred cross-shore circulation was found to be sensitive to the coordinate system selected. Using nominal (along-coast) coordinates, the average cross-shore current was found to be directed offshore within a surface layer which deepened with distance from the coast out to the shelf break, showed strong vertical shear only near the surface, and was divergent in the upper water column and convergent in the lower water column over the shelf. Current fluctuations about the local mean were strongly polarized along isobaths near the coast and became largely isotropic far from shore except offshore from Point Arena, where squirts were recurrently observed.

INTRODUCTION

Over the past 2 decades, moored current meters have been used to study the current field in coastal upwelling regions (for recent reviews see, for example, *Brink* [1983], *Huyer* [1983], *Allen* [1980], and *Winant* [1980]). Although these instruments provide a well-resolved picture of the time behavior of currents at isolated points, they only can provide limited subsampling of the spatial structure.

Figure 1 shows a schematic picture of the upwelling circulation which has been developed to explain such measurements off Oregon [*Huyer*, 1983]. This model is essentially two-dimensional; that is, it assumes that the important exchange processes occur in a cross-shore plane and that alongshore variability is much weaker than cross-shore variability. Equatorward wind forcing is expected to drive warm surface water offshore in an Ekman boundary layer. Below this layer, cold dense water flows toward the coast, surfacing in a band alongshore. Near the surface, the alongshore currents form a baroclinic equatorward jet, whose vertical shear is geostrophically balanced by cross-shore density gradients induced by the upwelling. At greater depth the alongshore currents reverse and form a poleward undercurrent flowing counter to the direction of wind forcing. Models of this circulation usually assume that the flow is linear, e.g., that gradients in velocity are much smaller than the Coriolis parameter [*Allen*, 1980].

Paper number 6C0539.
0148-0227/87/006C-0539$05.00

By contrast with the simple two-dimensional structure described above, the spatial structure in synoptically measured distributions of water properties is often found to be quite complex. Satellite images of sea surface temperature show that cold upwelled water does not occur in a uniform band along the coast [*Bernstein et al.*, 1977]. Regions of locally intense upwelling, called upwelling centers, have been observed in many locations [see *Brink*, 1983]. Tongues of cold water extending several hundred kilometers out to sea have been recognized along the west coast of the United States [*Traganza et al.*, 1981; *Breaker and Gilliland*, 1981]. Similar complex distributions of chlorophyll have been seen in satellite images of ocean color [*Abbott and Zion*, 1985]. However, little was directly known about the strength or structure of the circulation which forms such features. If they are associated with strong currents, they may represent important pathways of exchange between coastal and offshore waters.

During the Coastal Ocean Dynamics Experiment (CODE) a shipboard Doppler acoustic log (DAL) was used to directly measure and map the field of upper ocean currents over the northern California shelf and slope at points along the ship's track. The results of this mapping effort are reported below. The following section describes the DAL data set and processing. The results from several typical synoptic surveys are then discussed. These surveys reveal a close correspondence between the rich spatial structure in the satellite imagery and surprisingly vigorous, coherent flow structures at mesoscales and smaller scales. The paper concludes with a discussion of the structure in the averaged current fields over the shelf and inner slope.

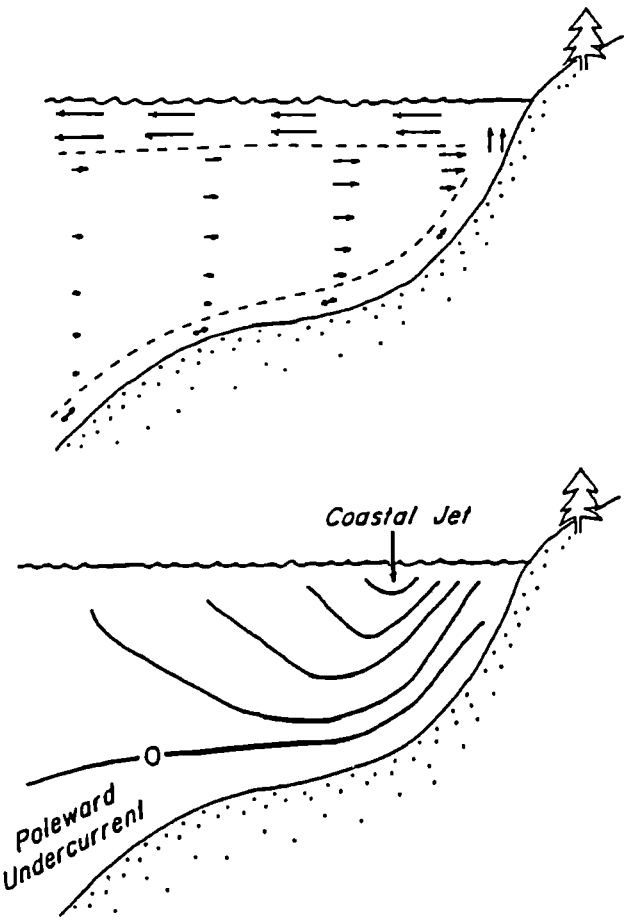

Fig. 1. Schematic of coastal upwelling circulation off Oregon [from *Huyer*, 1983].

DATA

The data for this study are shipboard measurements of horizontal ocean currents, obtained from continuous ship's drift estimates using a 300-kHz Ametek-Straza shipboard Doppler acoustic log to measure the vector velocity of the ship with respect to the ocean and a Northstar LORAN-C receiver to measure the velocity of the ship with respect to the earth. The system provided vertical profiles of horizontal ocean currents at the ship's location. Measurements in each profile were separated vertically by 6.5 m and typically spanned the depth range from 15 m to 150 m in deep water; over the shelf, only measurements within the upper 87% of the water column were used in order to reject potential bottom reflections of acoustic beam side lobes. Estimates of the currents were obtained by filtering the combined DAL and navigation (LORAN-C) data over 30 min. Comparison of shipboard current measurements processed in this way with those from vector measuring current meters moored over the shelf and slope during CODE showed differences with standard deviations of 5 cm s^{-1}; correlations between the shipboard and moored measurements were 0.95–0.97 for the energetic alongshore component of the currents and 0.76–0.82 for the generally weaker cross-shore component. The data-processing techniques, an error analysis, and the comparison with measurements from moored current meters are discussed in detail by *Kosro* [1985].

Some 74 days of shipboard current measurements were collected in the coastal and offshore waters of northern California during the spring and summer upwelling seasons of 1981 and 1982. The data were obtained continuously during drifter and mooring deployments, hydrographic surveys, and transit operations from the R/V *Wecoma*. The primary hydrographic grid (Figure 2) was also used for several drifter deployments and consisted of five cross-shore transects designated Elk, Arena, North, Central, and Ross from north to south. These lines were perpendicular to 0°, 338°, 320°, 320° and 320°T respectively. Adjacent transects were separated by about 25 km alongshore, and a survey of these lines required about $2\frac{1}{2}$ days to complete with conductivity, temperature, and depth (CTD) sampling. During each cruise, one complete survey and several partial surveys were usually obtained.

Surveys were conducted during a variety of wind conditions (Figure 3). Following the spring transition, surface wind forcing at midshelf in the CODE region was generally toward the southeast (upwelling favorable), with magnitudes of about 1–3 dyn cm^2. No strong downwelling favorable wind stress was observed during any post-transition cruise. In order to focus on coastal dynamics during the upwelling season, data obtained in 1982 prior to the spring transition in mid-April will not be included in the analysis.

SURVEYS

The results of seven individual mapping surveys are presented in Figures 4–7 below. This sample of the full data set was selected to give a "flavor" of the types of phenomena found in the CODE region. The results of two larger scale surveys have been reported by *Kosro and Huyer* [1986], and *Kosro* [1985] presents additional maps. The maps strongly corroborate the results presented by *Davis* [1985*a*], revealing that a "typical" current field contains much more spatial variability than was expected for two-dimensional upwelling (Figure 1) and that this structure is reflected in the distributions of sea surface temperature seen in satellite imagery. The vertical structure of the observed current features is also shown using current sections along selected transects.

The maps are constructed from shipboard measurements of the currents at 28-m depth. For clarity, measurements separated by less than a minimum distance (typically 4 km) have been averaged. The currents have been overlaid on satellite advanced very high resolution radiometer (AVHRR) images of sea surface temperature whenever relatively cloud-free images, close enough in time to the ship surveys, were available from the Scripps Remote Sensing Facility. Figure 2 can be used to relate the features seen to the bathymetry, and Figure 3 shows the local wind forcing during each survey. A detailed synthesis with the hydrographic measurements taken during these surveys is presented by *Huyer and Kosro* [this issue]. The purpose here is the same as *Davis*' [1985*a*], that is, to display features observed in maps of coastal currents, as an exercise in flow visualization.

Squirts and Eddies

The conceptual field (Figure 1) anticipates a flow dominated by an alongshore coastal jet. Offshore flow is expected to be uniform and weak; for a typical CODE wind stress (Figure 3) of 1 dyn cm^2, the expected offshore current would

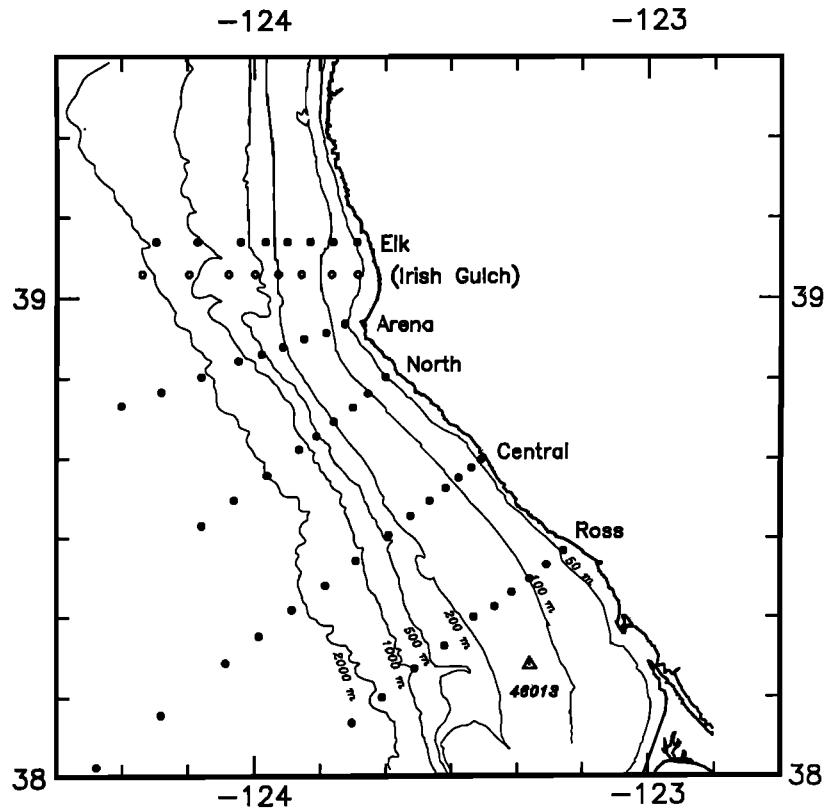

Fig. 2. Primary grid of CTD stations for CODE, along which most shipboard current measurements were made. The Irish Gulch line was sampled by CTD only during 1982. The 1982 Central line was shifted 3 km south of the 1981 line shown. The position of wind buoy NDBO 46013 is marked by a triangle.

average 5 cm s^{-1} over an Ekman layer 20 m thick. However, the synoptic maps of observed currents (Figures 4 and 5) often reveal narrow bands along the coast of greatly enhanced offshore flow that are also observed in drifter records from the same period. *Davis* [1985*a*] has called these features "squirts".

The earliest mapping survey, conducted from April 26 to 28, 1981, revealed the presence of a vigorous squirt, about 20 km wide, centered about 25 km south of Point Arena (Figure 4*a*). The peak seaward current exceeded 50 cm s^{-1} at the 28-m depth shown. Cold water dyes a portion of the squirt, but both an underway thermistor record and the satellite image suggest that the squirt at 28-m depth is somewhat broader than the surface tongue of cold water.

The strong vertical and horizontal shears in this squirt can be seen in the current sections of Figures 4*b* (along the squirt) and 4*c* (across the squirt). The vertical integral of the currents is clearly seaward (toward 220°T) everywhere over

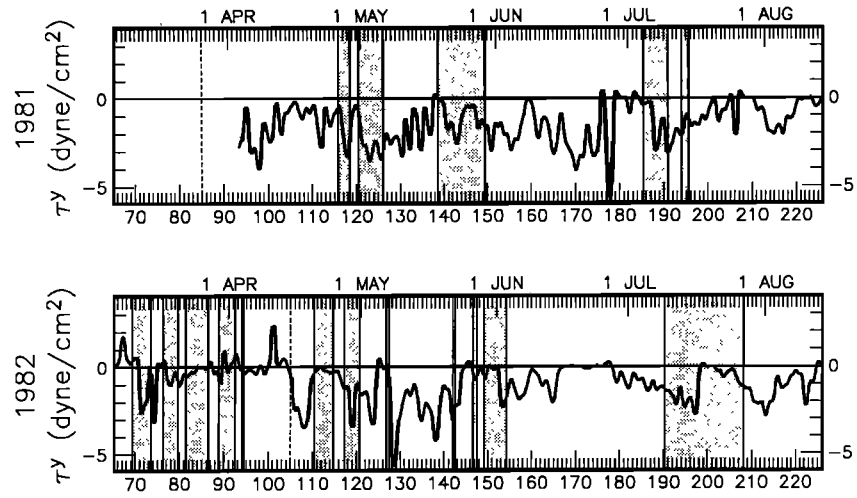

Fig. 3. Alongshore component (toward 317°T) of surface wind stress (in dynes per square centimeter at midshelf in the southern CODE region. Periods of shipboard surveys are shaded. The time of spring transition to upwelling conditions is indicated by a dashed line. Hourly wind velocity data from NDBO 46013 (see Figure 2) were converted to stress and low passed using a filter with a 40-hour half power point.

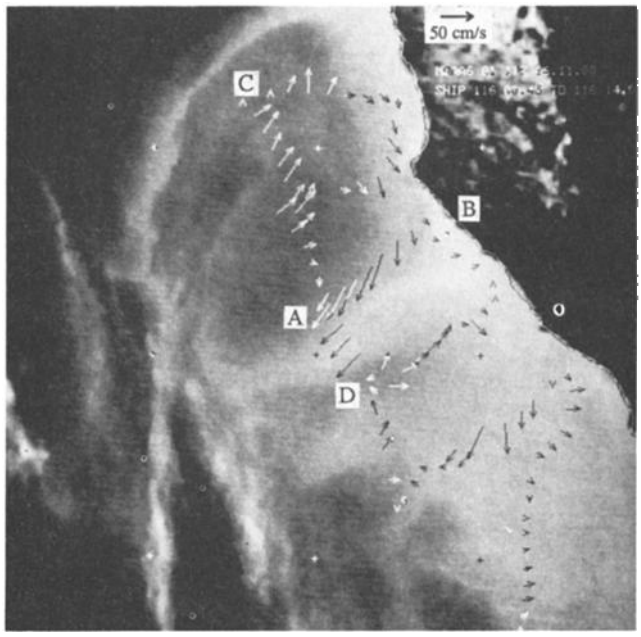

Fig. 4*a*. Shipboard current measurements from 28-m depth, plotted over NOAA 6 AVHRR image of sea surface temperature (colder water has lighter grey shades). Shipboard survey results are from 0045 UT on April 26 through 1400 UT on April 28, 1981; the satellite image is from 1611 UT on April 27, 1981. Tick marks are placed every 30 min of latitude and longitude; Point Arena (38°57′ N, 123°44′ W) provides a landmark. The velocity scale is shown by the arrow at upper right.

the shelf along the squirt axis (Figure 4*b*). Thus in this feature, mass balance is not achieved as expected in two-dimensional upwelling (Figure 1), by compensating shoreward flow at depth; there must be onshore flow further north or south and convergence of the alongshore flow toward the squirt. The transect across the squirt does, in fact, show flow toward the coast in the warm water north of the squirt. Integration of the DAL currents through the transect in Figure 4*c* yields approximately balancing cross-shore mass transports over the upper 180 m, with ~1.8 Sv flowing onshore in the northern half of the section and ~1.6 Sv flowing seaward in the southern half. Coincident hydrographic measurements of dynamic topography [*Fleischbein et al.*, 1982] confirm that the geostrophic flow is shoreward in the north and seaward in the south but averages to zero over the transect from Elk to Central lines.

Streamers of cold water driven offshore by strong, highly sheared currents appear often in the CODE data (Figures 5*a*–5*d*). A week after the survey shown in Figure 4, the region was resurveyed (Figure 5*a*) during a period of strong wind forcing (Figure 3). Even though the observed flow for this survey conformed more with classical expectations, with currents polarized alongshore over most of the shelf, the currents split off Point Arena, one branch turning offshore and again carrying upwelled water away from the coast. Surface drifters deployed in a line off Point Arena dramatically echoed this observation (see Figure 5 of *Davis* [1985*a*]). Strong narrow current features are also observed well away from the coast; nearly 100 km from shore, such currents can be seen deforming the temperature field in the southern portion of the survey (38.0°N, 124.9°W).

Figure 5*b* makes it clear that energetic eddies centered over the continental slope can reach onto the shelf and deform the temperature field, sweeping upwelled water away from the shelf and even recirculating it back again. This survey appears to show a pair of counterrotating eddies, separated alongshore, whose shoreward limbs merge off Point Arena.

Figures 5*c* and 5*d* show two maps of the temperature and current fields obtained 5 days apart in mid-July 1982. Figure 5*d* is at the inshore end of one survey described in detail by *Kosro and Huyer* [1986]. Although substantial variability, both spatial and temporal, was evident in the wind field during this period [*Huyer et al.*, 1984; *Beardsley and Alessi* 1985], strong features are observed in the currents, measured over several days, which correspond well to features in the sea surface temperature, measured in minutes by the satellite. The image of July 14–16, 1982 (Figure 5*c*) shows two cold tongues and the associated current features. The northern tongue is swept out to sea along the southern edge of a strongly sheared current which hugs the coast north of Point Arena. The southern tongue exhibits weaker flow along its axis and weaker shear across it. Five days later, following the period of calm winds, the July 19–22 survey (Figure 5*d*) shows that the southern tongue and the currents associated with it have disappeared. A cyclonic eddy between the two cold tongues can be inferred from the IR and is clearly seen in the current measurements. This eddy, centered about 35 km from shore over the continental slope, dominated the currents [*Kosro*, 1985] and dynamic topography [*Huyer et al.*, 1984] south of Point Arena at least from July 16 to 22, and one surface drifter [*Davis*, 1983] was trapped by the eddy for nearly 8 days, completing 3 circuits around its core.

Wind Relaxations

Periods of light or zero winds often alternated with periods of strong equatorward wind forcing in the CODE region (Figure 3). The flow during these wind "relaxations" has proven to be quite interesting. Unfortunately, low clouds and fog often accompany these events, obscuring satellite images. Three surveys obtained during wind relaxations are shown in Figures 6*a*–6*c*; however, only one satellite image is available (the same image was used for both Figure 6*a* and 6*b*).

The surveys from April 1982 provide well-defined examples of the current field during a wind relaxation. Following sustained equatorward winds which commenced on April 14, 1982, and apparently triggered the spring transition [*Huyer et al.*, 1979] to the upwelling dynamical regime in the CODE region [*Lentz*, this issue], the winds over the entire CODE 2 array calmed dramatically on April 19 and remained calm

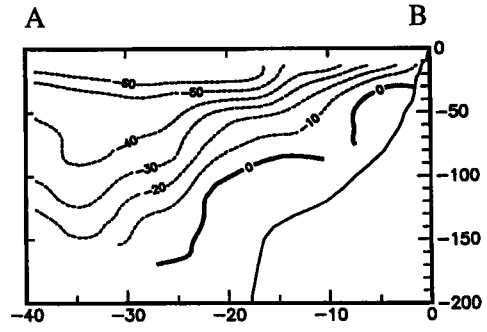

Fig. 4*b*. Vertical section of seaward current (positive toward 220°T) from the survey of Figure 4*a*: onshore-offshore transect taken from point A to point B (along the North line).

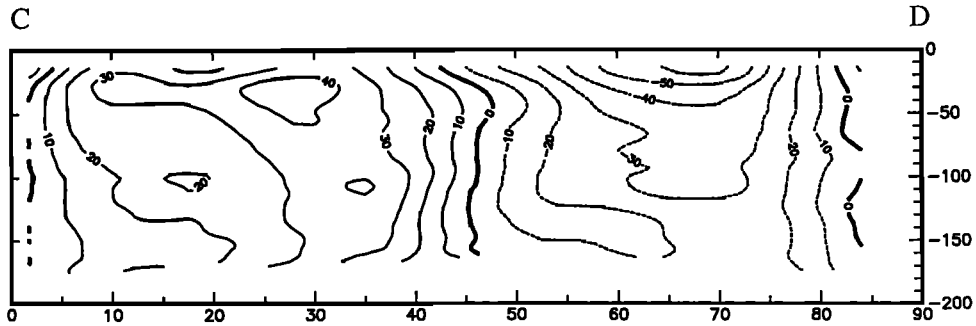

Fig. 4c. Vertical section of seaward current (positive toward 220°T) from the survey of Figure 4a: alongshore transect from point C to point D (about 45 km from shore between the Elk and Central lines).

until April 25. The coastal current field was mapped by shipboard DAL during April 20–24. The satellite image from this period (Figures 6a and 6b) shows a wedge of warm surface water close to the coast, with cooler water lying offshore. Simultaneous hydrographic measurements [*Fleischbein et al.*, 1983] show that the warm surface water is accompanied very close to shore by a thin layer of low salinity. The Russian River, flowing at an average rate of 105 m^3 s^{-1} during this period [*Markham et al.*, 1984] is a likely source for the fresh water [see *Huyer and Kosro,* this issue].

The observed flow field is remarkable (Figures 6a and 6b). Near the coast, strong poleward flow is associated with the band of warm water. This flow occurs in the absence of any significant wind forcing. Farther offshore a strong equatorward jet is present. This flow is strongly polarized in the alongshore direction, unlike those of Figures 4 and 5. From late May to very early June 1982, a subsequent wind relaxation (Figure 3) was accompanied by a similar nearshore wedge of poleward flow (Figure 6c).

The vertical structure of the alongshore flow across a series of CTD transects covering a 36-hour period is shown in Figure 7a, displayed from north to south. Nearshore poleward flow is observed in each transect, albeit strongly reduced at the Irish Gulch line north of Point Arena. The observed cyclonic horizontal shear is strongest along the Arena line, where $\partial v/\partial x$ is somewhat larger than the Coriolis parameter f. The observed vertical shear structure is interesting. The poleward flow is relatively barotropic, while the offshore zone shows strong vertical shear of -10^{-2} s^{-1} and more. This suggests that the nearshore zone is barotropically forced, as by an alongshore sea level gradient. The barotropic component of the flow can not be determined hydrographically. As a result, the surface dynamic height maps from this period fail to detect the poleward flow near the coast [*Fleischbein et al.*, 1983].

The persistence of the strong structures discussed here is also noteworthy. During this cruise, the Central line was surveyed four times. Figure 7b, which shows offshore profiles of the alongshore current at 28-m depth for each survey, shows that the poleward flow persisted for more than 3 days, its cross-shelf profile changing very little within 20 km of the coast (the equatorward jet in v, beyond 25 km from shore, apparently sharpened somewhat between the second and third surveys).

Discussion

The DAL current measurements, when viewed as maps, show considerably stronger spatial structure than was expected. Could this structure simply be aliasing of temporal variability, despite the apparent connection with features in the surface temperature field? If the structure is real, how isotropic is it? These issues are addressed below.

Synopticity. The shipboard surveys each took about 2–3 days to complete. As a result, the current measurements will contain contributions from internal and inertial waves, tides, and other high-frequency oscillations. As the ship travels, these oscillations will be aliased into spatial structure. If the high-frequency oscillations have both large energy and large correlation lengths, then maps will be badly aliased; if the oscillations have either low energy or correlation lengths which are short in comparison with the spatial filtering used, the shipboard maps will be good representations of the synoptic field.

To determine the time scales of the energetic patterns of current variability, spatial empirical orthogonal functions (EOFs) were determined from the CODE 2 hourly moored current meter data from 35-m depth and the (integral) decorrelation times [*Davis*, 1976] calculated for the time varying amplitudes of each EOF. As was expected, the more energetic modes have larger spatial scales, while the less energetic modes contain the shorter scale structures. Time scales for the energetic modes were also longer. The first four EOFs explain 79% of the total variance (48%, 19%, 7%, and 6%, respectively) and have an energy-weighted time scale of 4.8 days (3.5, 9.5, 2.5, and 2.4 days respectively). The coastal DAL surveys shown above were completed in about half this time, while the average time separating pairs of measurements, $\langle | t_j - t_{i \neq j} | \rangle$ ranged from less than one eighth to about one fourth of the decorrelation time. Thus although the DAL surveys are not a snapshot, the features seen are much more indicative of spatial structure than temporal variability.

The following discussion of the structure function of the current field provides additional evidence for the synopticity of the maps presented above.

Scales. From the combined sea surface temperature and current maps of Figures 4–6, the impression might be left that the synoptic current field over the shelf varies as much alongshore as its does across shore. However, observations from moored current meters off Oregon and Washington [*Huyer et al.*, 1975] have found that coherence lengths are much longer alongshore than cross shore. For the DAL data set, a statistical measure of the scales of variability in the currents can be obtained from a calculation of the structure function, defined to be simply the mean squared difference

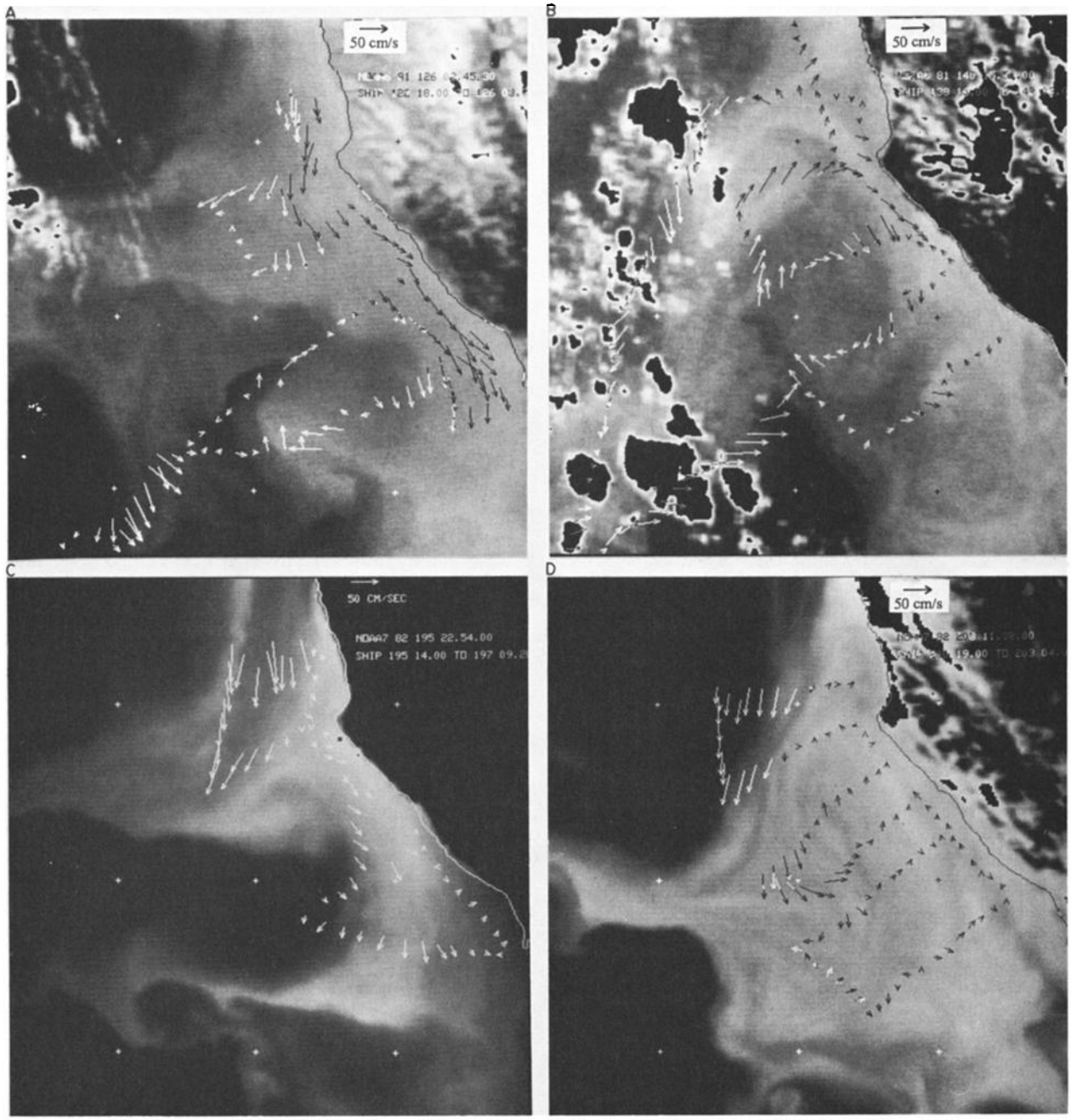

Fig. 5. Survey results as in Figure 4*a* (*a*) from 1800 UT on May 2 through 0330 UT on May 6, 1981, with a satellite image from 0345 UT May 6, 1981; (*b*) from 1600 UT on May 18 through 0300 UT on May 22, 1981, with a satellite image from 1550 UT on May 20, 1981; (*c*) from 1400 UT on July 14 through 0920 on July 16, 1982, with a satellite image from 2254 UT on July 14, 1981; and (*d*) from 1900 UT on July 19 through 0400 UT on July 22, 1982, with a satellite image from 2259 UT on July 22, 1982.

between currents measured at different times or locations, as a function of temporal or spatial lag,

$$D(\Delta x, \Delta y, \Delta t) = \langle [\mathbf{u}(x, y, t) - \mathbf{u}(x + \Delta x, y + \Delta y, t + \Delta t)]^2 \rangle$$

Note that for a stationary, homogeneous field,

$$\tfrac{1}{2} D(\Delta x, \Delta y, \Delta t) = C(0, 0, 0) - C(\Delta x, \Delta y, \Delta t)$$

where $C(\Delta x, \Delta y, \Delta t)$ is the space- and time-lagged covariance and thus $C(0, 0, 0)$ is the variance.

Structure functions of the current field at 20-m depth south of Point Arena were estimated independently from the shipboard current measurements and from the CODE 2 moored array. For each reasonably complete shipboard survey, maps of currents at 20-m depth were prepared, the quasi-spatial structure function over each map was calculated, and the results were accumulated over maps and averaged. As in Figures 4–6, current measurements separated by less than 4 km were averaged. To concentrate on shelf processes, only data taken in water less than 200 m deep were used in the calculation. For the moored array, simultaneous current measurements from the nine instruments at 20-m depth and one (N3) at 35-m depth were used to calculate $D(\Delta x, 0, 0)$ and $D(0, \Delta y, 0)$; the hourly current

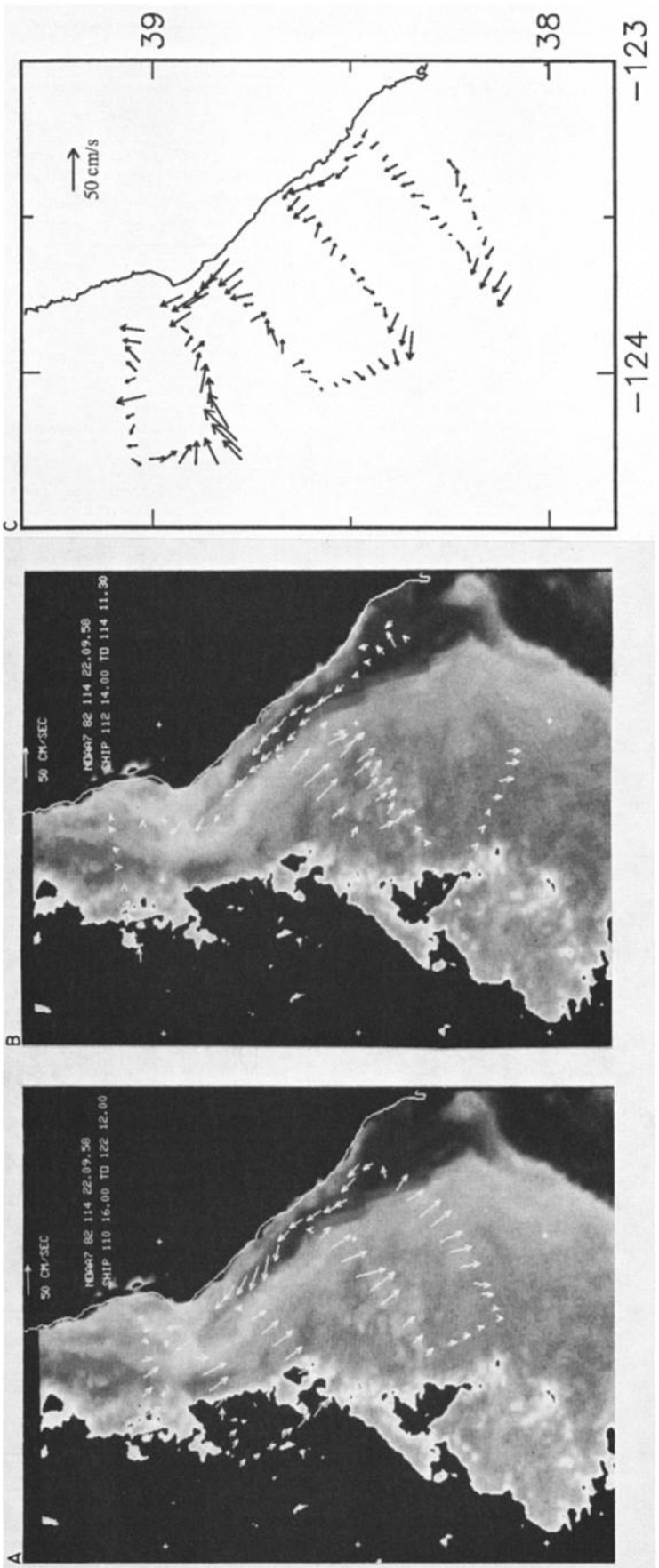

Fig. 6. Survey results as in Figure 4*a* (*a*) from 1600 UT on April 20 through 1200 UT on April 22, 1982, with a satellite image from 2210 UT on April 24, 1982 (note time delay of the satellite image from the survey and that the labeled time is incorrect); (*b*) from 1400 UT on April 22 through 1130 UT on April 24, 1982, with a satellite image from 2210 UT on April 24, 1982 (same image as Figure 6*a*), and (*c*) from 0630 UT on May 29 through 0436 UT on May 31, 1982 (no satellite image).

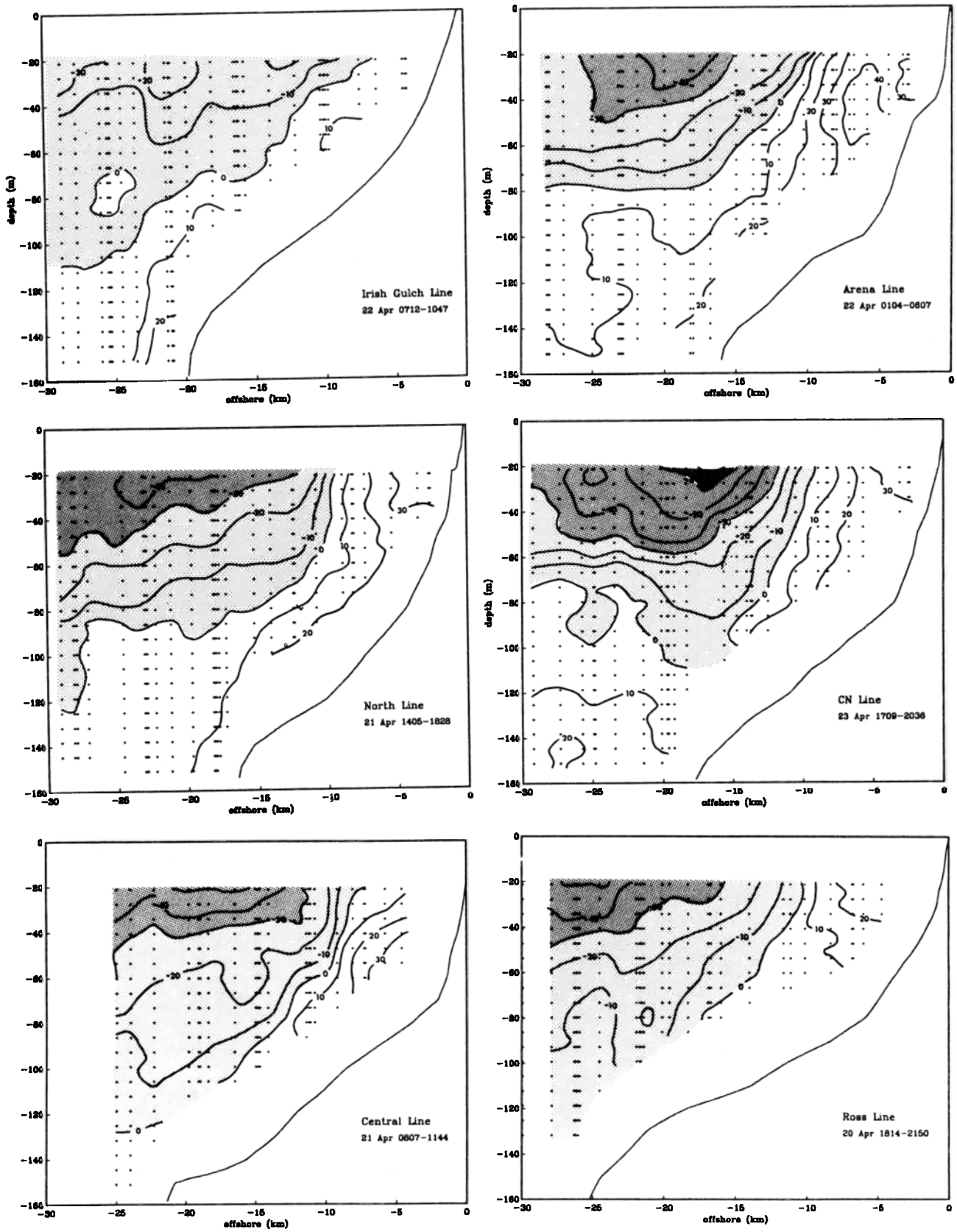

Fig. 7*a*. Alongshore currents during wind relaxation, April 20–24, 1982. Sections are from the five primary CTD lines plus the CN line midway between the Central and North lines. Dots show locations of measurements. The contour interval is 10 cm s^{-1}. Equatorward currents are shaded.

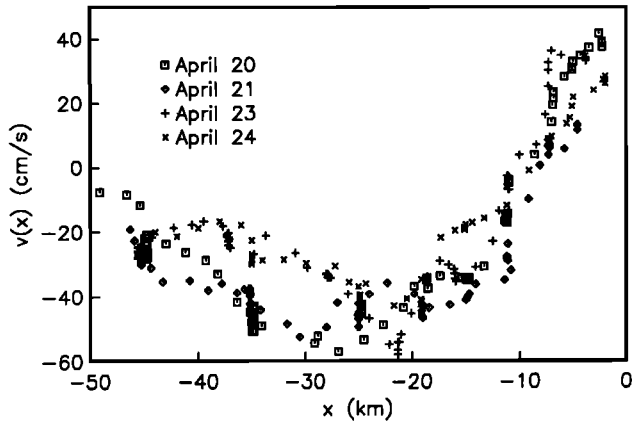

Fig. 7*b*. Alongshore current $v(x)$ at 28-m depth versus offshore distance x for four transects of the Central line during April 20–24, 1982.

measurements were time-lagged to calculate $D(0, 0, \Delta t)$ at each of these 10 instruments, and the results were then averaged.

The results of these calculations are shown in Figure 8. The points to stress about Figure 8 are that (1) the spatial mean square difference profiles obtained with the moored instruments are very similar to those obtained with the shipboard sampling and (2) both indicate that mean square difference grows much more rapidly with cross-shore separation than with alongshore separation. The latter indicates that cross-shore scales are substantially shorter than alongshore scales, in agreement with expectations from other locations but surprising in view of the synoptic maps of Figures 4–6. The former indicates that the structure function for data taken over several days' sampling is not greatly different from the structure function obtained from simultaneous data. The averaging over 4 km in the shipboard data appears to have suppressed the high-frequency fluctuations in the currents, leaving primarily spatial structure. The fact that there is such small difference between the filtered DAL results, obtained over several days, and the moored instrument results, which are simultaneous measurements, shows that spatial variability within a survey is much larger than temporal variability during a survey and even suggests that substantial variance seen at a fixed current meter is due to advection of spatial structure.

AVERAGES

Maps of the average current at 15-m depth, expected error in the average, and standard deviation of the fluctuations (Figures 9*a* and 9*b*) were prepared from measurements at CTD station locations sampled at least 8 times during the 1981 and 1982 upwelling seasons. At each station, data separated by less than 1 day in time were averaged and treated as a single occupation. Fluctuations are shown as principal axis ellipses in Figure 9*b*; error ellipses (Figure 9*a*) are the fluctuation ellipses scaled by $1/\sqrt{N}$, where $8 \leq N \leq 34$ is the number of occupations at each station. No spatial smoothing between stations has been done.

The map of average current (Figure 9*a*), while somewhat noisy owing to the limited number of samples, shows the features expected in a coastal upwelling region. At 15 m the average currents over the shelf have magnitudes up to 25 cm s^{-1}. The largest component of the flow over the shelf is along coast, in the direction of the mean wind forcing (except at the shallowest station along the Central line, where the average is poleward). Although poorly resolved because of limited sampling, a much smaller, generally offshore, cross-isobath component can also be seen, suggesting that the waters at this depth are in the wind-driven Ekman layer. The along coast component shows a tendency to increase with distance from the coast, reach a maximum value near the shelf edge, and then decrease again farther offshore, that is, to form a mean coastal jet.

As was found off Oregon [*Kundu and Allen*, 1976], fluctuations about the mean value (Figure 9*b*) are strongly polarized in the alongshore direction near the coast, while farther from shore the fluctuations become more nearly isotropic. Over the shelf the direction of polarization rotates offshore in the same sense as the isobaths. This rotation is especially pronounced off Point Arena, where the alongshore direction changes sharply; there, fluctuations quickly become strongest in a direction which is distinctly across isobaths. This is the statistical signature of the squirts which were recurrently observed off Point Arena (Figures 4 and 5).

The vertical structure of the averaged current fields along the five primary CTD lines is shown in Figures 10*a*–10*c*. Here currents have been resolved into nominally cross-shore and alongshore components $u(x, z)$, $v(x, z)$, where the alongshore direction $\hat{y}$ is taken to be 0°T for the Elk line, 338°T for the Arena line and 320°T for the North, Central and Ross lines. Data were preaveraged along each line in space-time bins of extent $(\Delta x, \Delta z, \Delta t) = (2.5 \text{ km}, 6.5 \text{ m}, 1 \text{ day})$, and then averaged across time at each CTD line. The jetlike structure in the alongshore flow is clearly visible in the

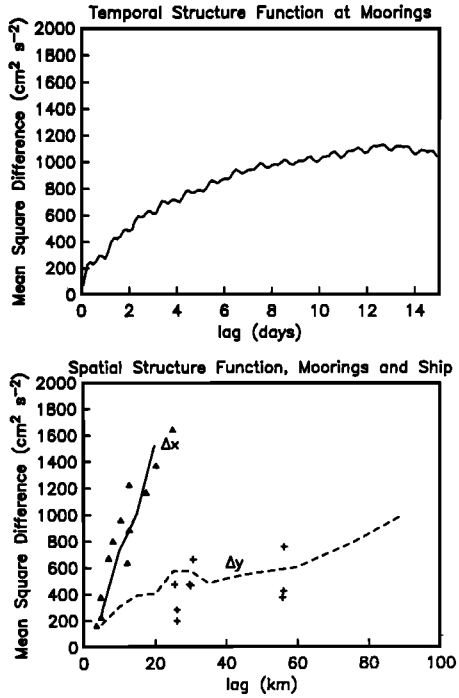

Fig. 8. Structure function (mean squared difference between field values as function of spatial or temporal lag) of shelf currents at 20-m depth from current meter and shipboard data. Upper panel shows structure function versus temporal lags only, from moored instruments. Lower panel shows estimates of structure function versus cross-shore lag (shipboard data, solid line; current meter data, triangles) and alongshore lag (shipboard data, dashed line; current meter data, plusses).

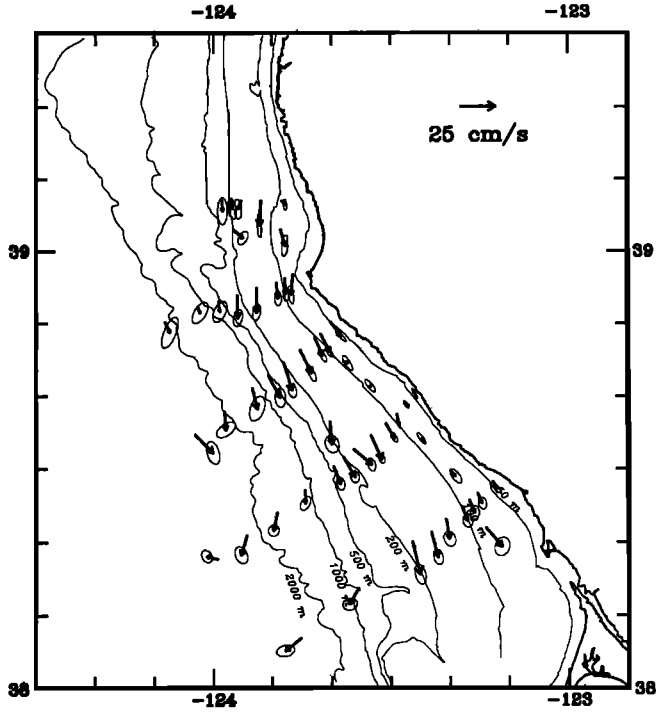

Fig. 9*a*. Average current measured at 15-m depth at each CTD station location. Station locations were occupied at least 8, and up to 34, times during upwelling seasons of 1981 and 1982. Ellipses shows the 1 standard error uncertainty in each average.

average sections. The core of the jet appears to accelerate and move offshore as the shelf broadens from north to south. At greater depth, the alongshore component of the current reverses, giving way to a poleward undercurrent. The average cross-shore component of the flow is weak and generally not well resolved from line to line, as can be seen from the estimates of standard error (Figure 10*b*). Along the Central line, where the number of samples is fairly large, some evidence of a surface Ekman layer can be detected, with offshore flow near the surface and onshore flow at greater depth.

To achieve better resolution of the structure in the flow, the sampling noise must be reduced through additional averaging. Figures 11*a*–11*c* show the field and error estimates when all CTD lines are averaged together as functions of offshore distance and depth. Many of the model features expected for a coastal upwelling flow field off Oregon (Figure 1) become evident in the averaged fields in the CODE region. Consistent with the observed equatorward mean wind stress, a near surface layer of offshore transport is evident at all offshore locations in Figure 11b. The thickness of this layer increases from less than 20 m near the coast to about 50 m near the shelf break. Weak onshore flow occurs everywhere below this layer, except in a region over the shelf near the bottom of the DAL resolution (where the difference from zero is generally not significant). It is this pattern of cross-shore circulation which produces the upwelling of cold water near the coast. Near the surface, the averaged alongshore flow is characterized by an equatorward jet extending from midshelf to beyond the shelf break. Flowing counter to the equatorward mean wind stress, a poleward undercurrent, strongest near the shelf break, surfaces near the coast.

Fluctuations in u and v about their average values (Figure 11*c*) are at least as large as the averges themselves. Far from shore, the fluctuations in u and v are equally energetic. As the coast is approached, the fluctuations in u are damped dramatically.

Vertical gradients in the mean fields were computed by smoothing first differences between adjacent (x, z) bins with a (3 × 3) triangular weight filter. The results are shown in Figure 12. The shear field for $\bar{u}$ shows the depth extent of the directly wind driven layer particularly well. In the interior, away from surface and bottom stresses, the vertical shear in $\bar{u}$ is small (generally less than 10^{-3} s^{-1}). Above 40 m, $\bar{u}$ becomes increasingly sheared as the surface is approached, as can be expected in the presence of wind forcing. For $\bar{v}$, by contrast, substantial vertical shear is evident over a much greater depth range, as can be expected if the upwelled density surfaces are geostrophically balanced. Agreement between measured $\partial\bar{u}/\partial z$ and prediction based on steady surface Ekman dynamics (Figure 13) is good in deep water; departures from prediction are largest in shallow water as the bottom is approached.

Horizontal profiles of $\bar{u}$ at fixed depths across the shelf (Figure 14) show that significant divergence ($\partial\bar{u}/\partial x > 0$) is present in near-surface currents over the entire shelf, while deeper in the water column the average cross-shelf flow converges toward the coast ($\partial\bar{u}/\partial x < 0$). In the upper water column over the shelf, the cross-shore divergence averages 3 × 10^{-6} s^{-1}; this agrees with *Davis*' [1985*b*] estimate of surface divergence from drifter measurements. If the divergence in the alongshore current can be neglected, mass conservation and the data in Figure 14 imply that the mean vertical (upwelling) current will be directed toward the surface, with a maximum where $\partial\bar{u}/\partial x = 0$. Although the DAL data do not reach the surface or the bottom, integration over the data available suggests a mean upwelling rate at the midwater maximum of at least 0.7 × 10^{-2} cm s^{-1}, or 6 m day^{-1}, averaged over the inner 15 km of shelf. The implied vertical mass transport over this part of the shelf would be

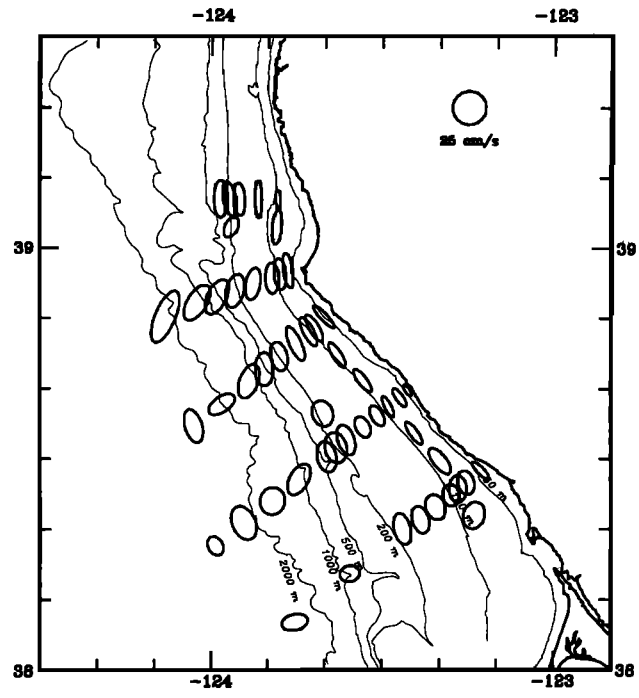

Fig. 9*b*. Standard deviation of current fluctuations, resolved along principal axes. at each CTD location.

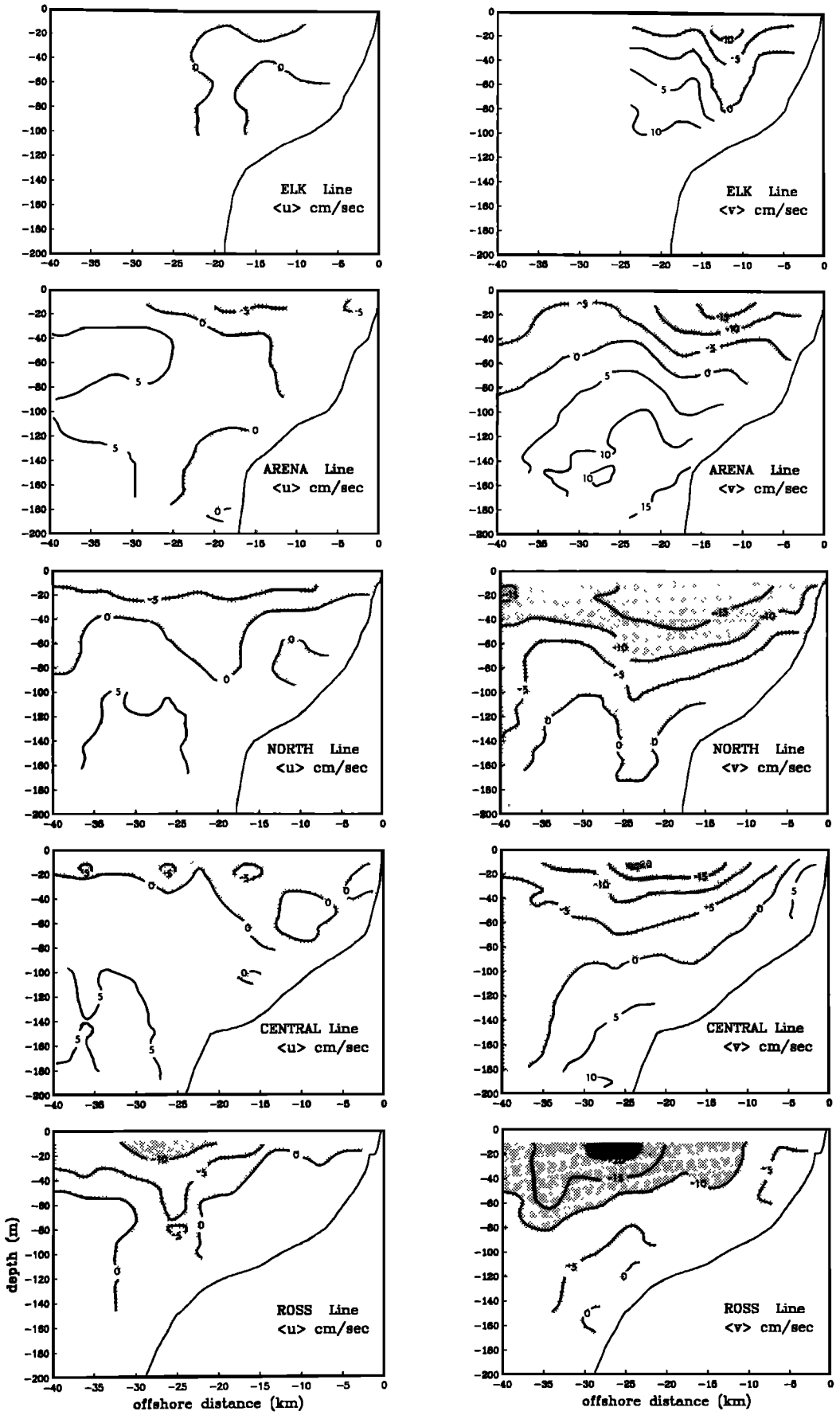

Fig. 10*a*. Sections of average cross-shore and alongshore current components at each primary CTD line in Figure 2.

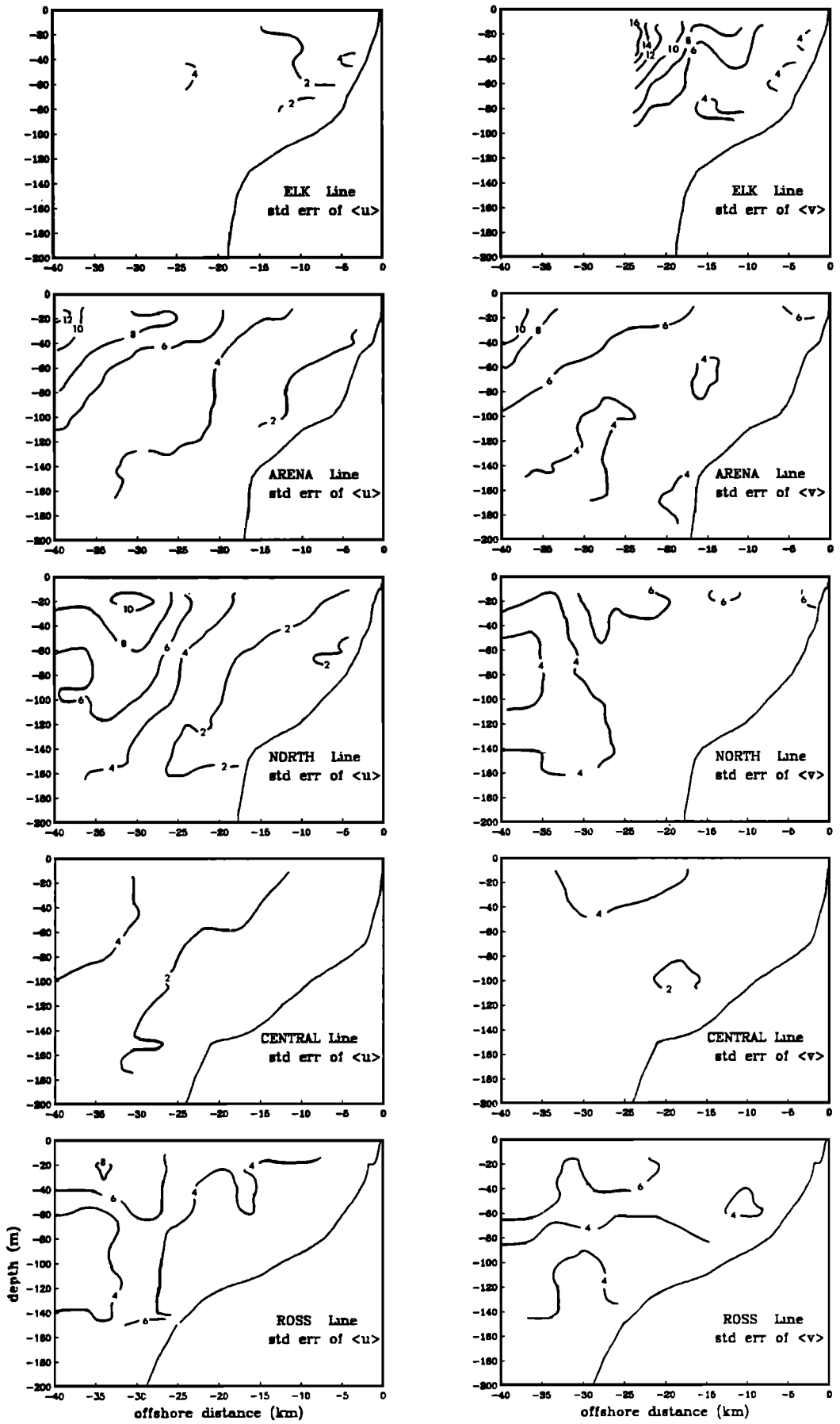

Fig. 10*b*. Uncertainty (1 standard error) in average currents of Figure 10*a*.

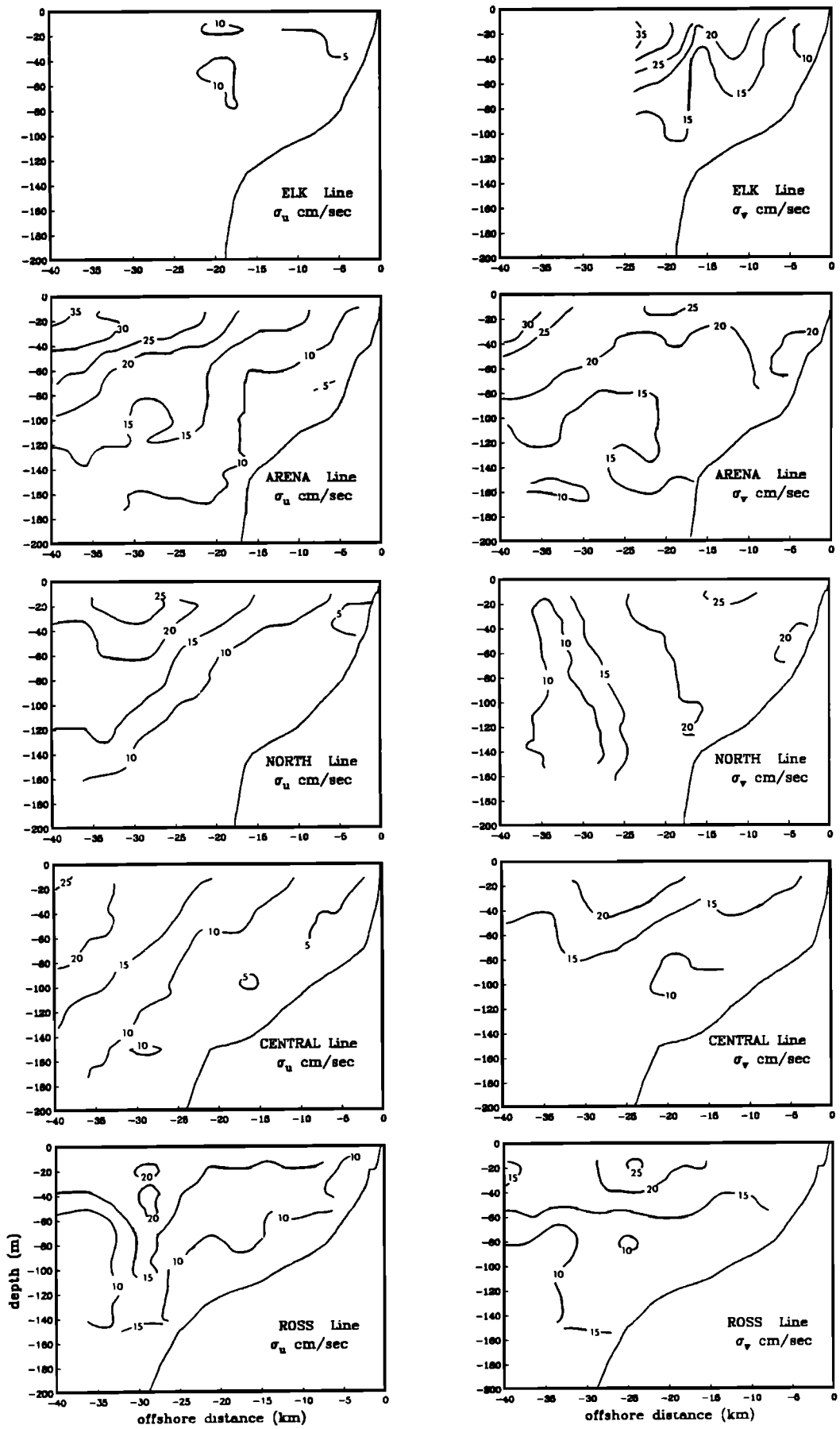

Fig. 10*c*. Standard deviation of fluctuations in average current components at each primary CTD line in Figure 2.

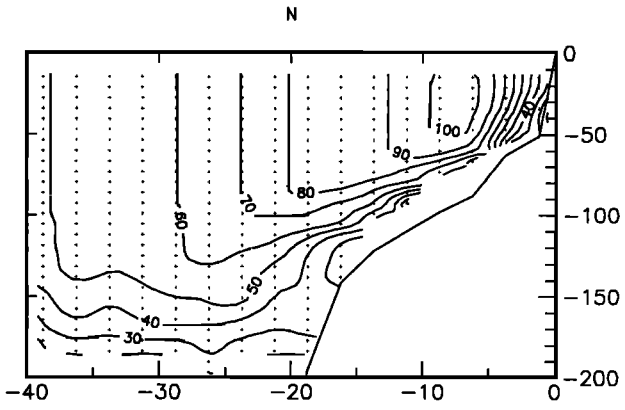

Fig. 11*a*. Number of observations in each averaging bin for Figures 11*b* and 11*c*. Each observation was made along one of the primary CTD lines in Figure 2. Center depth and offshore location of each bin are shown by a cross. Bins with less than 20 observations were not used in averages.

about 10^5 m^2 day^{-1}, an amount equal to the offshore Ekman transport forced by a mean surface wind stress of 1 dyn cm^{-2}.

The alongshore structure in the mean field (Figure 10*a*) implies a nonzero $\partial\bar{v}/\partial y$, negative onshore (positive offshore) of the core of the jet, which contributes to the total divergence responsible for the mean upwelling. Because the core of the jet migrates offshore, $\partial\bar{v}/\partial y$ is a function of the alongshore coordinate y. The effect of $\partial\bar{v}/\partial y$ is to increase substantially the inferred maximum $\bar{w}$ over the shelf and to decrease it beyond the shelf break.

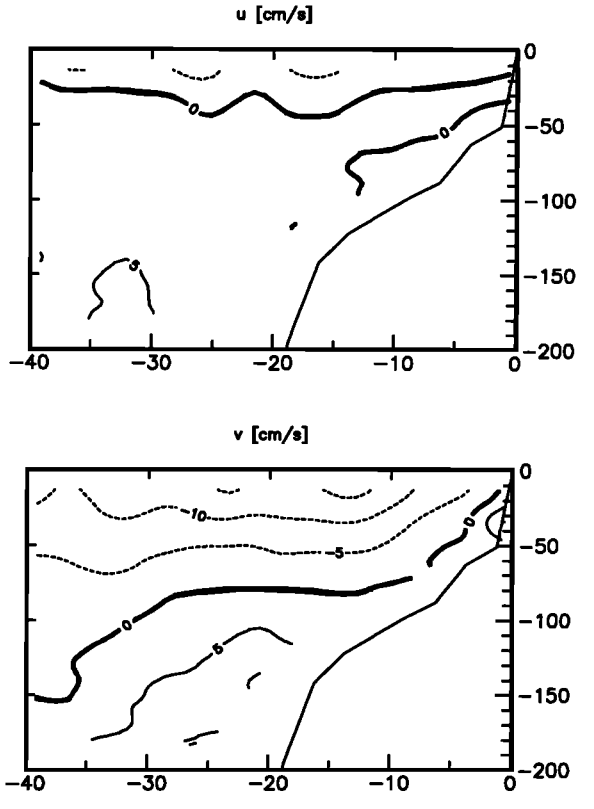

Fig. 11*b*. Average currents in the (top) cross-shore and (bottom) alongshore directions.

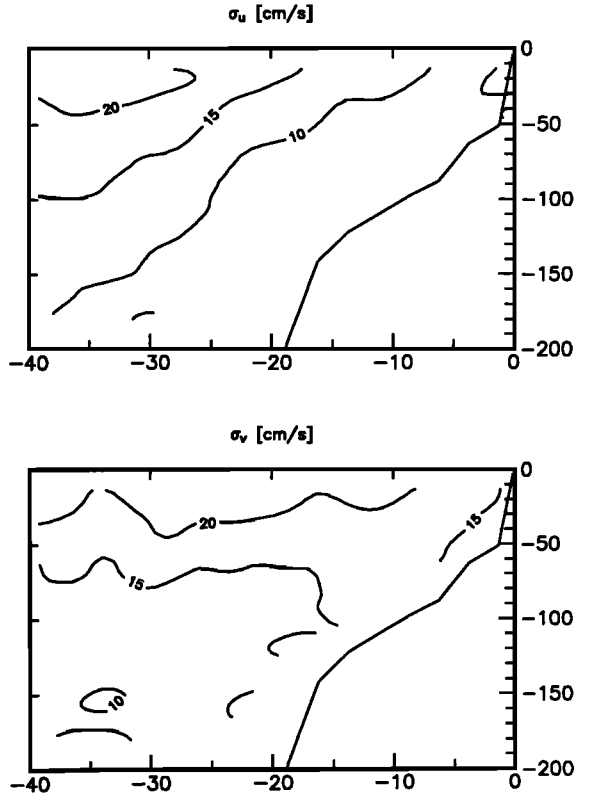

Fig. 11*c*. Standard deviation of fluctuations in $\bar{u}, \bar{v}$ (in centimeters per second).

Significant divergence in $\bar{u}$ is also present in the vicinity of the deep maximum in $\bar{u}$ near the shelf break (Figure 11*b*); whether this result represents true physics or simply an overoptimistic estimate of statistical reliability is not known. The limited evidence from the moored instruments at C5 do show an increase in $\bar{u}$ in this region.

Discussion and Summary

The shipboard current measurements provide a view of the mean circulation which is very well sampled in space but not continuously sampled in time. It is apparent from Figure 3 that especially during 1982, sampling may be biased toward periods of low winds. The bias in the mean currents due to shipboard sampling of the wind forcing was estimated at each CTD station from a simple regression analysis of the moored current measurements on the wind stress at NDBO 46013. The predicted bias was small and did not significantly affect the structure of the fields presented above.

In Figure 11, averages of the current field were computed as $\bar{u}(x, z)$ and $\bar{v}(x, z)$, where x, z are the distance from shore and depth below the surface respectively. However, because the shelf width doubles between Point Arena and the Ross line, such averaging will produce horizontal smearing of current features that follow isobaths. Figure 15 shows that when the averages are computed as $\bar{u}(H, z)$, $\bar{v}(H, z)$, where H is the water column depth, the near-surface jet in the alongshore currents is brought into sharper focus; the structure in the cross-shore currents is rather insensitive to this change.

Trying to resolve the average cross-shore flow raises serious questions of coordinate system definition. It has long been recognized that because $\bar{u}$ is substantially weaker

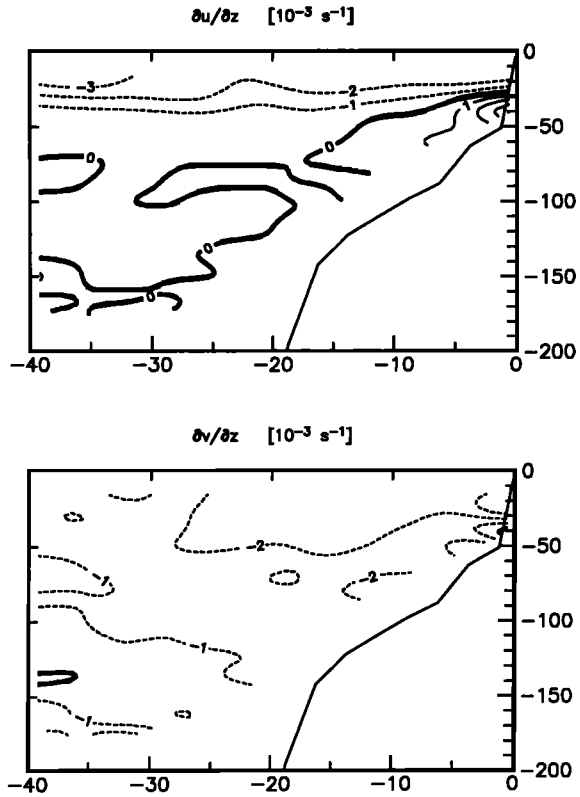

Fig. 12. Vertical shear in $\bar{u}, \bar{v}$ (10^{-3} s^{-1}). First differences of the averaged fields (Figure 11*b*) were smoothed using a 3 × 3 triangular weight filter.

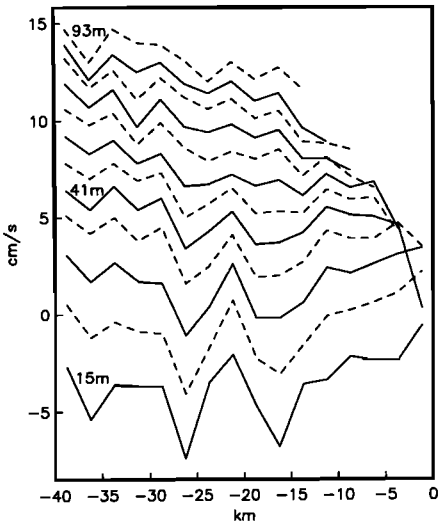

Fig. 14. Plot of $\bar{u}(x)$ at a series of depths. Shallowest data are at 15 m, deepest data are at 93 m. For clarity, data from successive depths have been offset by 1 cm s^{-1} from preceding depths. Note divergence in shallow $\bar{u}$ over shelf and convergence in deeper $\bar{u}$.

than $\bar{v}$, it is difficult to select a definition of the alongshore direction that avoids mapping some of the structure of $\bar{v}$ into $\bar{u}$.

Three definitions of alongshore direction θ were tested to resolve the average cross-shore circulation: (1) nominal directions, set by CTD lines, (2) a modified principal axis system, and (3) a zero mean cross-shore transport system.

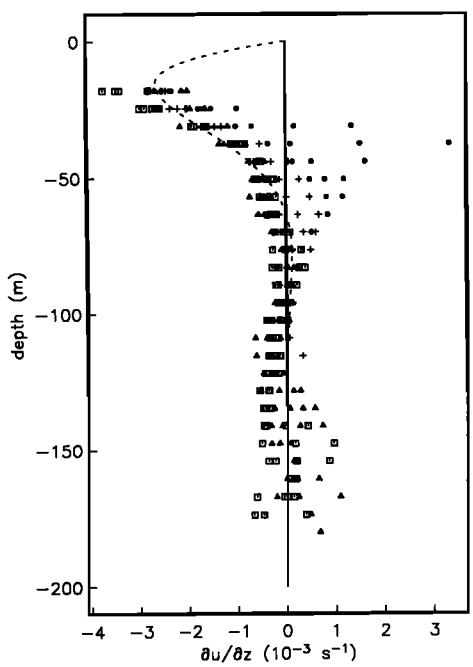

Fig. 13. Comparison of measured $\partial\bar{u}/\partial z$ (10^{-3} s^{-1}) with surface Ekman layer prediction (dashed line). Measured averages are segregated into four classes by offshore location: 0–10 km (dots), 10–20 km (plusses), 20–30 km (triangles), and 30–40 km (squares) from shore. The Ekman profile assumes a steady alongshore wind stress of −1.5 dyn cm^{-2}, an Ekman layer depth $(2A_v/f)^{1/2}$ = 20 m, and an infinitely deep ocean.

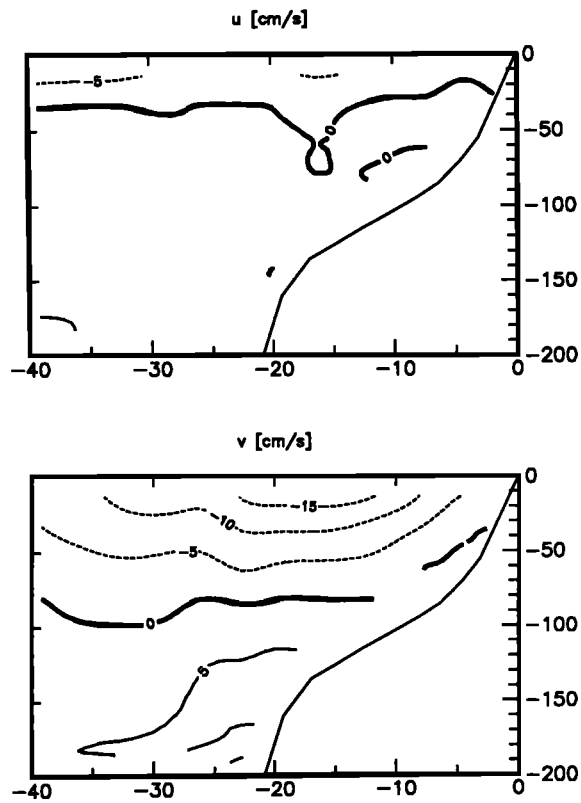

Fig. 15. Average current which results when data are placed in bins according to water column depth rather than offshore distance. The offshore coordinate shown is the average over data in the given water column depth bin. The alongshore jet is better resolved in these along-isobath coordinates.

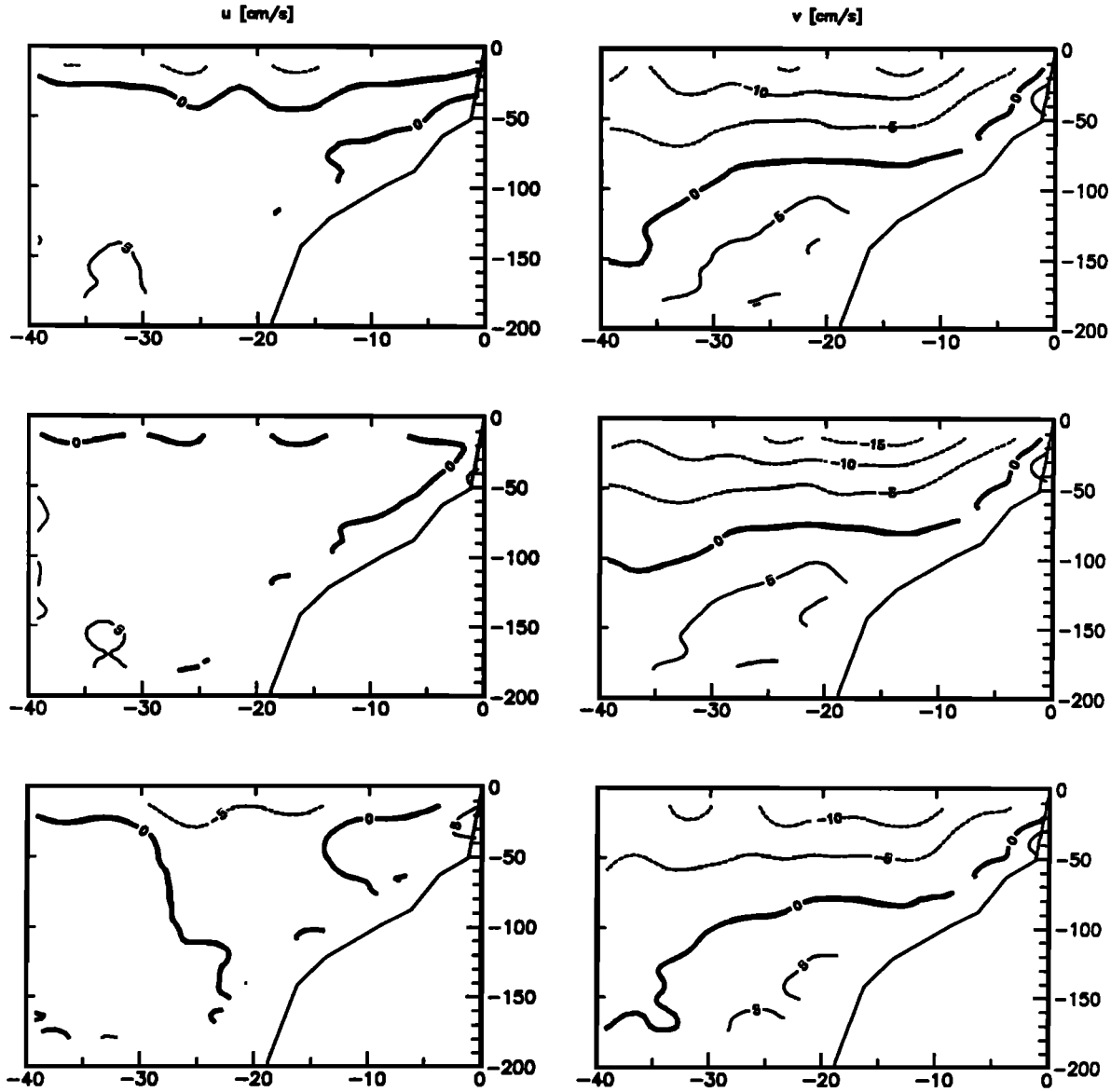

Fig. 16. Effect of various definitions of alongshore direction on component averages. Data were processed as for Figure 11*b* except that before averaging between CTD lines, the current averages were resolved into alongshore and cross-shore components, where the alongshore direction was selected to be (top pair) perpendicular to the CTD transect as in Figure 11*b*, (middle pair) along the spatial principal axis of the mean currents, or (bottom pair) perpendicular to the direction of zero mean transport.

An average over realizations of $(u(x, z), v(x, z))$ was calculated in nominal coordinates for each CTD line (nominal CTD line directions were initially selected subjectively to generally cross isobaths). For definition 1 these data were then averaged with no further rotation. For definition 2, $\langle \bar{u}\bar{u} \rangle$, $\langle \bar{v}\bar{v} \rangle$, and $\langle \bar{u}\bar{v} \rangle$ were found along each line (angle brackets indicate averaging over x, z). Before averaging between lines, the means were rotated to a coordinate system for which $\langle \bar{u}\bar{v} \rangle = 0$, that is, one for which the spatial structure in u is forced to be uncorrelated with the spatial structure in v. This represents an attempt to require that none of the structure in the alongshore flow gets mapped into the cross-shore flow. For definition 3 the area integrals of u and v over depth and offshore distance were calculated for each section, and the rotation angle for each section was determined for which the integral of u was forced to zero.

TABLE 1. Alongshore Angle θ and Counterclockwise Rotation Angle $\Delta\theta$ From Nominal for Coordinate Systems Based Upon Modified Principal Axis Scheme and no Cross-Shore Transport Scheme for Defining Cross-Shore Direction

Line	Nominal θ	Principal Axis θ	Principal Axis $\Delta\theta$	Zero Mean U θ	Zero Mean U $\Delta\theta$
Elk	0.0	3.8	−3.8	17.5	−17.5
Irish Gulch	0.0	2.5	−2.5	42.5	−42.5
Arena	338.0	341.9	−3.9	18.8	−40.8
North	317.0	341.6	−24.6	308.5	8.5
Central	317.0	335.9	−18.9	272.2	44.8
Ross	317.0	346.7	−29.7	325.6	−8.6

The results of the calculation are summarized in Figure 16 and in Table 1. The alongshore flows change very little with various definitions of θ; the major features of a strongly vertically sheared, surface-intensified alongshore flow, about 15 cm s^{-1} equatorward at the surface, 0 cm s^{-1}

between 80- and 100-m depth, and poleward at up to 10 cm s^{-1} below that, most intense at the shelf break, are retained with each rotation.

The cross-shore field, on the other hand, does change character considerably. The results obtained using definition 1, the nominal coordinate system, were discussed in the analysis of Figures 10–14. The results obtained using definition 2 or 3 do not seem to improve the resolution of the cross-shore flow. For definition 2 the principal axis system, the surface offshore flow is rather weak, and the structures of $\bar{u}$ and $\bar{v}$ are clearly distinct. However, the cross-shelf mass imbalance is much larger than it is for the nominal coordinates. For definition 3, where zero net cross-shelf transport is required, the results are unphysical, with onshore mean flow appearing over the inner shelf and offshore flow over the whole water column being found near the shelf break. This definition appears to have mapped a portion of the alongshore jet structure into the cross-shore currents in order to achieve cross-shore mass balance, a result probably due to the limited vertical range over which the DAL can obtain valid data. These results do point out, however, that for this data set the most reasonable cross-shelf flow field is obtained using the nominal coordinates from the CTD sections.

In summary, the dense spatial sampling provided by the shipboard DAL clearly delineates the extent and intensity of features in the coastal upwelling circulation. Synoptic maps show a current field which varies strongly in both x and y and which only rarely resembles the smooth conceptual field of Figure 1. Instead of occurring in a simple surface Ekman layer, large offshore transport of cold coastal water is frequently seen in very active regions of short horizontal scale. A jet in the alongshore current, the most prominent feature seen in the conceptual field, is seen only occasionally in the individual maps. Strong current fluctuations are present at a wide range of scales, and coherent eddylike structures centered beyond the shelf break carry water upwelled at the coast far out to sea. Despite this strong alongshore variability, the near-surface currents over the shelf vary more rapidly cross shore than alongshore. The average circulation, by contrast, exhibits many features expected in a two-dimensional upwelling circulation. The mean cross-shelf circulation shows an Ekman layer of offshore transport near the surface with return flow below. Out to the shelf break, this layer of mean offshore flow deepens with distance from the coast. A poleward undercurrent is clearly seen in the mean alongshore current; it appears strongest near the shelf break, and it surfaces near the coast. A near-surface equatorward jet is apparent in the mean alongshore current across each hydrographic line, but since its core moves offshore from north to south, it is artificially smoothed out when means are calculated as a function of offshore distance alone. The currents show significant divergence in both alongshore and cross-shore components, from which the mean vertical current can be calculated. Mean upwelling appears to occur over the entire shelf, providing enough vertical transport to balance the predicted mean Ekman transport in the CODE region. Fluctuations about the mean current are strongly polarized in the alongshore direction near the coast and essentially isotropic far from the coast. However, flow offshore from the coastal corner at Point Arena shows fluctuations polarized away from the coast, a signature of the squirts recurrently found there in the synoptic fields.

Acknowledgments. This work would not have been possible without the contributions of R. E. Davis and L. A. Regier. R. Beardsley, A. Dorkins, J. Fleischbein, N. Pettigrew, D. Rudnick, R. Schramm, and C. Winant helped collect portions of the Doppler data set. Additional data were provided by R. E. Davis, R. Beardsley, C. Winant, J. Allen, and G. Halliwell. The contributions of A. Huyer and P. Flament are gratefully acknowledged. This work was funded by the National Science Foundation under grants OCE-8410546 and OCE-8410861 and by the Office of Naval Research under grant N00014-80-C-0440.

REFERENCES

Abbott, M. R., and P. M. Zion, Satellite observations of phytoplankton variability during an upwelling event, *Cont. Shelf Res.*, *4*, 661–680, 1985.

Allen, J. S., Models of wind-driven currents on the continental shelf, *Annu. Rev. Fluid Mech.*, *12*, 389–433, 1980.

Beardsley, R. C., and C. A. Alessi, An array description of the surface wind and near-surface currents, CODE-2 Moored Array and Large Scale Data Report, *Tech. Rep. 85-35*, edited by R. Limeburner, pp. 109–132, Woods Hole Oceanogr. Inst. Woods Hole, Mass., 1985.

Bernstein, R. L., L. Breaker, and R. Whritner, California Current eddy formation: Ship, air and satellite results, *Science*, *195*, 353–359, 1977.

Breaker, L. C., and R. P. Gilliland, A satellite sequence on upwelling along the California coast, in *Coastal Upwelling, Coastal and Estuarine Sci.*, vol. 1, edited by F. A. Richards, pp. 87–94, AGU, Washington, D.C., 1981.

Brink, K. H., The near-surface dynamics of coastal upwelling, *Prog. Oceanog.*, *12*, 223–257, 1983.

CODE Group, Coastal ocean dynamics, *Eos Trans. AGU*, *64*, 538–540, 1983.

Davis, R. E., Predictability of sea surface temperature and sea level anomalies over the North Pacific Ocean, *J. Phys. Oceanogr.*, *6*, 249–266, 1976.

Davis, R. E., Current-following drifters in CODE, *Ref. 83-4*, 73 pp., Scripps Inst. of Oceanogr., La Jolla, Calif., 1983.

Davis, R. E., Drifter observations of coastal surface currents during CODE: The method and descriptive view, *J. Geophys. Res.*, *90*, 4741–4755, 1985*a*.

Davis, R. E., Drifter observations of coastal surface currents during CODE: The statistical and dynamical views, *J. Geophys. Res.*, *90*, 4756–4772, 1985*b*.

Fleischbein, J., W. E. Gilbert, and A. Huyer, Hydrographic data from the first Coastal Ocean Dynamics Experiment: Leg 4, 25 April–7 May 1981, *Ref. 82-2*, 149 pp., School of Oceanogr., Oreg. State Univ., Corvallis, 1982.

Fleischbein, J., W. E. Gilbert, and A. Huyer, Hydrographic data from the second Coastal Ocean Dynamics Experiment: R/V *Wecoma*, Leg 6, 18–24 April 1982, *Ref. 83-4*, 130 pp., School of Oceanogr., Oreg. State Univ., Corvallis, 1983.

Huyer, A., Coastal upwelling in the California current system, *Prog. Oceanogr.*, *12*, 259–284, 1983.

Huyer, A., and P. M. Kosro, Mesoscale surveys over the shelf and slope in the upwelling region near Point Arena, California, *J. Geophys. Res.*, this issue.

Huyer, A., B. M. Hickey, J. D. Smith, R. L. Smith, and R. D. Pillsbury, Alongshore coherence at low frequencies in currents observed over the continental shelf off Oregon and Washington, *J. Geophys. Res.*, *80*, 3495–3505, 1975.

Huyer, A., E. J. Sobey, and R. L. Smith, The spring transition in currents over the Oregon continental shelf, *J. Geophys. Res.*, *84*, 6995–7011, 1979.

Huyer, A., J. Fleischbein, and R. Schramm, Hydrographic data from the second Coastal Ocean Dynamics Experiment: R/V *Wecoma*, Leg 9, 6–27 July 1982, *Ref. 84-7* , 130 pp., School of Oceanogr., Oreg. State Univ., Corvallis, 1984.

Kosro, P. M., Shipboard acoustic current profiling during the Coastal Ocean Dynamics Experiment, Ph.D. thesis, *SIO Ref. 85-8*, 119 pp., Scripps Inst. of Oceanogr., La Jolla, Calif, 1985.

Kosro, P. M. and A. Huyer, CTD and velocity surveys of seaward jets off northern California, July 1981 and 1982, *J. Geophys. Res.*, *91*, 7680–7690, 1986.

Kundu, P. K., and J. S. Allen, Some three-dimensional character-

istics of low-frequency current fluctuations near the Oregon coast, *J. Phys. Oceanogr.*, *6*, 181–199, 1976.

Lentz, S. J., A description of the 1981 and 1982 spring transitions over the northern California shelf, *J. Geophys. Res.*, this issue.

Markham, K. L., V. Piro, W. F. Shelton, and M. W. Weston, Jr., Water resources data for California, Water year 1982, vol 2, Pacific slope basins from Arroyo Grande to Oregon state line except Central Valley, 417 pp., Water Resour. Div., U.S. Geol. Surv., Reston, Va., 1984.

Traganza, E. D., J. C. Conrad, and L. C. Breaker, Satellite observations of a cyclonic upwelling system and giant plume in the California Current, in *Coastal and Estuarine Sci.*, vol. 1, edited by F. A. Richards, pp. 228–241, AGU, Washington, D.C., 1981.

Winant, C.D., Coastal circulation and wind-induced currents, *Annu. Rev. Fluid Mech.*, *12*, 271–301, 1980.

P. M. Kosro, College of Oceanography, Oregon State University, Corvallis, OR 97331.

(Received May 13, 1986;
revised September 1, 1986;
accepted September 15, 1986.)